Optimized Noise Filtration through Dynamical Decoupling

Hermann Uys,[1,2] Michael J. Biercuk,[1,3] and John J. Bollinger[1]

[1]*National Institute of Standards Technology, 325 Broadway, Boulder, Colorado 80305, USA*
[2]*Council for Scientific and Industrial Research, Brummeria, Pretoria, South Africa*
[3]*Georgia Institute of Technology, Atlanta, Georgia, USA*

(Received 31 March 2009; published 20 July 2009)

Recent studies have shown that applying a sequence of Hahn spin-echo pulses to a qubit system at judiciously chosen intervals can, in certain noise environments, greatly improve the suppression of phase errors compared to traditional dynamical decoupling approaches. By enforcing a simple analytical condition, we obtain sets of dynamical decoupling sequences that are designed for optimized noise filtration, but are independent of the noise spectrum up to a single scaling factor set by the coherence time of the system. These sequences are tested in a model qubit system, $^9Be^+$ ions in a Penning trap. Our combined theoretical and experimental studies show that in high-frequency-dominated noise environments with sharp high-frequency cutoffs this approach may suppress phase errors orders of magnitude more efficiently than comparable techniques can.

DOI: 10.1103/PhysRevLett.103.040501 PACS numbers: 03.67.Pp, 03.65.Yz, 37.10.Ty, 76.60.Lz

Developing improved strategies for maintaining quantum coherence in the presence of environmental noise is central to the advancement of quantum control experiments and applications. The fields of quantum computation and information processing stand to gain significantly from such strategies. One approach to maintaining coherence consists of applying simple pulses intermittently [1–5] with computational control operations. Similarly, it is possible to design the computationally relevant control operations themselves with the same objective in mind [6–8]. These techniques are commonly referred to as dynamical decoupling. One widely used scheme entails applying a sequence of Hahn spin-echo-style π pulses [9], successive pulses being separated by free-precession delays. The precise durations of these interpulse delays that would provide optimum error suppression is currently a topic of many research efforts [3–5,10]. The Uhrig dynamical decoupling (UDD) sequence [3,5] has shown especially promising improvements over traditional approaches such as Carr-Purcell-Meiboom-Gill (CPMG) multipulse spin echo [11] in certain noise environments.

In this Letter we devise and test the noise-suppression capabilities of dynamical decoupling pulse sequences tailored for optimized noise filtration (OFDD sequences). To that end, we enforce a simple analytical condition that does not depend on detailed knowledge of the noise spectrum, yielding, up to a scaling factor in time, a set of optimized pulse sequences. Each member of the set of sequences is optimized for a unique choice of sequence duration and consequently each member has different relative pulse locations. In that sense the concomitant dynamical decoupling may be thought of as being "locally optimized" [12]. This should be contrasted with most other spin-echo-style dynamical decoupling, e.g., UDD, in which analytical considerations [3] naturally lead to fixed relative pulse locations for all sequence durations.

Our studies demonstrate that OFDD sequences suppress errors comparably to, or better than, sequences with fixed relative pulse locations in arbitrary noise environments, making orders of magnitude gains in noise environments with strong high-frequency components and sharp high-frequency cutoffs. The sharpness of the cutoff that allows improvement over CPMG by UDD was studied in [5]. In low-frequency-dominated noise environments OFDD performs similarly to CPMG which is an effective slow-noise filter. Finally, we demonstrate the efficacy of phase-error suppression by testing OFDD sequences using trapped ions as a model system, showing strong agreement between theory and experiment.

We consider the time evolution of a two-level system (qubit) under the influence of random classical noise that causes an instantaneous deviation in frequency, $\beta(t)$, from the unperturbed qubit frequency, Ω. The dynamics of the qubit are governed by the Hamiltonian: $\hat{H} = \hbar/2[\Omega + \beta(t)]\hat{\sigma}_z$, where $\hat{\sigma}_z$ is the Pauli spin operator parallel to the quantization axis. We adopt the following conventions for a decoupling sequence of n π pulses: let τ be the total dynamical decoupling sequence duration, equal to the sum of the free-precession delays between pulses, plus the sum of all π-pulse durations. If the center of the jth π pulse occurs at time $t = t_j$ then let $\delta_j = t_j/\tau$ and let each π pulse have duration τ_π. Assuming the qubit spin vector is initially aligned along the y axis we use the expectation value of $\hat{\sigma}_y$ in the frame rotating at frequency Ω as a measure of coherence $W(\tau) = |\overline{\langle\sigma_y(\tau)\rangle}| = e^{-\chi(\tau)}$, where $\chi(\tau)$ is the coherence integral, $\chi(\tau) = \frac{2}{\pi}\int_0^\infty S(\omega)\frac{F_n(\omega\tau)}{\omega^2}d\omega$ [3–5]. The angle brackets in the former indicate the quantum mechanical expectation value and the overline an ensemble average. $S(\omega)$ is the power spectral density of $\beta(t)$, ω is the angular frequency, and $F_n(\omega\tau)$ [12,13] a filter function dependent on the n π-pulse locations

$$F_n(\omega\tau) = \left|1 + (-1)^{n+1}e^{i\omega\tau} + 2\sum_{j=1}^{n}(-1)^j e^{i\omega\delta_j\tau}\cos(\omega\tau_\pi/2)\right|^2. \quad (1)$$

Tailoring the filter function by choosing appropriate δ_j can lead to enhanced suppression of dephasing.

The coherence integral is smallest, and hence the error suppression strongest, when the overlap between the noise power spectrum and the filter function is minimized. Thus we enforce the condition that the area under the filter function $A_F(\tau)$ be minimized over a relevant frequency domain $[0,\omega_D]$ where ω_D is a potentially unknown high-frequency cutoff. This area depends both on the relative pulse locations, δ_j, and the total sequence duration τ; as such, optimization yields a set of pulse sequences, each sequence optimized for a given value of τ. In the most general case $A_F(\tau)$ also depends on τ_π, but the following discussion focuses primarily on the instantaneous pulse approximation ($\tau_\pi = 0$), which is appropriate in qubit systems where π-pulse durations are small compared to the system's coherence time, e.g. [14,15].

Transforming to dimensionless units by defining $\omega' = \omega/\omega_D$ and $\tau' = \omega_D\tau$ we want $A_F(\tau') = \omega_D \int_0^1 F_n(\omega'\tau')d\omega'$ to be a minimum. No detailed knowledge of the noise spectrum enters into this condition and ω_D appears only as an overall scaling factor, so that the same set of sequences minimizes $A_F(\tau')$ for any ω_D. In practice, therefore, the same set of sequences can be used for any noise environment by scaling the duration of all sequences in the set by the same factor while maintaining the same relative pulse locations in each individual sequence.

For fixed τ' we determine the relative pulse locations that minimize $A_F(\tau')$ by running a numerical search routine. We use the UDD sequence as an initial guess at $\tau' = 0$ and the sequence obtained after convergence as the initial guess for the next choice of τ', and so on. In Figs. 1(a) and 1(b) we show the sets of OFDD sequences so obtained for a range of sequence durations and assuming, respectively, $n = 6$ and $n = 10$ instantaneous π pulses, symmetrically distributed around $0.5\tau'$.

The observation that the condition of minimized $A_F(\tau')$ yields a set of pulse sequences which provide near-optimum performance in any noise environment constitutes the central result of this work. These sequences lead to significant gains over existing ones in high-frequency-dominated noise environments as we show next.

We present simulations comparing the error suppression capabilities of OFDD sequences obtained by minimizing $A_F(\tau')$ only, to that of UDD and CPMG, as well as to sequences obtained by minimizing the spectrum dependent $\chi(\tau)$ directly (referred to as LODD—locally optimized dynamical decoupling [12]). In Figs. 2(a)–2(d) we plot simulations of the decoherence, $[1 - W(\tau')]/2$, having used $n = 6$ and $n = 10$ instantaneous π pulses, and a dimensionless spectrum $S(\omega')/\omega_D = \alpha\omega'^\gamma$, where α is the dimensionless noise strength. We chose two limiting cases to illustrate the range of possible outcomes when using OFDD sequences. Those are an Ohmic, $\gamma = 1$ (relevant to a spin-boson model for semiconductor quantum dots [5]), and a "$1/f$" ($\gamma = -1$) spectrum, respectively. We assume an infinitely sharp cutoff for the Ohmic, but for the $1/f$ spectrum a soft high-frequency cutoff $\sim\omega'^{-2}$ and a sharp low-frequency cutoff at $\omega' = 0.001$ (to prevent spectrum divergence as $\omega' \to 0$). The main features of this comparison are that, in the high-frequency-dominated noise environments, Figs. 2(a) and 2(b), the OFDD approach achieves superior error suppression over the entire

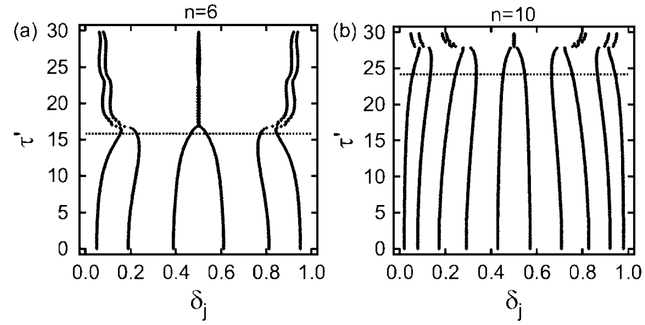

FIG. 1. OFDD sequences for (a) $n = 6$ and (b) $n = 10$ pulses. The horizontal axis indicates the pulse locations, δ_j, relative to the total sequence duration τ' (vertical axis) that minimize $A_F(\tau')$. The horizontal dashed line at (a) $\tau' = 15.8$ and (b) $\tau' = 24.2$ indicates when $F_n(\tau') = 1$. For longer sequence durations the system is largely dephased.

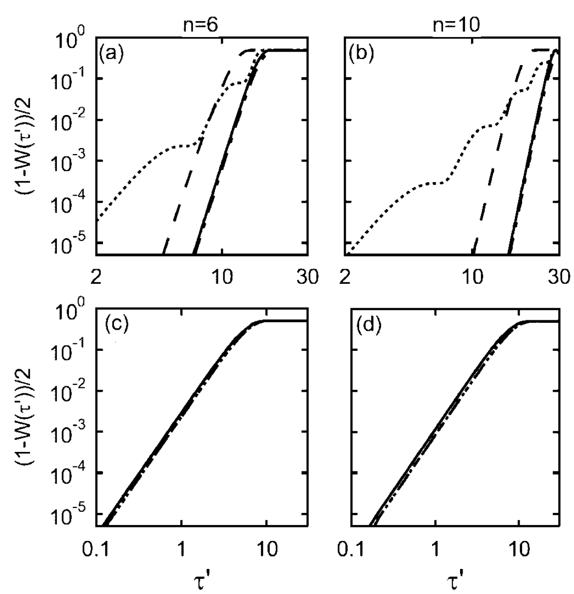

FIG. 2. Comparison of decoherence, $[1 - W(\tau')]/2$, due to phase errors when using $n = 6$ (left) and $n = 10$ (right) pulse CPMG (dotted lines), UDD (dashed lines), OFDD (solid lines), and spectrum dependent LODD (dot-dashed lines) in an (a), (b) Ohmic and (c),(d) $1/f$ noise environment, respectively. We assumed $\tau_\pi = 0$ and used $\alpha = 1$ throughout.

coherence time. The OFDD error curve has roughly the same polynomial growth as that of UDD, but extends the coherence time by a factor ~ 1.5. Our simulations show that these characteristics persist independently of the noise strength and pulse number up to ~ 20 π pulses, beyond which the optimization becomes numerically challenging. Note that the OFDD result differs from the LODD approach by a relative error of only a few percent (the two curves are nearly indistinguishable). In the low-frequency-dominated $1/f$ environment, Figs. 2(c) and 2(d), all four approaches perform similarly. We have verified that similar improvements occur for supra-Ohmic noise spectra ($\gamma > 1$) with sharp cutoffs, results are similar to CPMG for $\gamma < -1$, while intermediate benefits are achieved for white noise with a sharp cutoff. As a rough measure of what constitutes a "sharp" cutoff, we find empirically that significant benefits arise from our approach if the integrated noise power beyond a high-frequency peak is less than $\sim 10\%$ the total integrated noise power and contained within a frequency width one tenth of ω_D.

These numerical results motivate us to develop an experimental procedure for implementing OFDD sequences. To that end, consider the following analysis. The average relative delay between pulses is $\approx 1/n$. At times $\tau' \ll 1$ all the phase factors in Eq. (1) (within the domain $\omega' \epsilon [0, 1]$) are small compared to $\pi/2$, and the different contributions in the sum add destructively [in particular $F_n(0) = 0$]. At times $\tau' \gg 1$ the phase factors in successive terms in the sum can differ by order $\sim \pi$, and the terms in the sum may add constructively. The filter function then oscillates rapidly as a function of frequency around its average value $4n + 2$ and the system is largely dephased. The crossover between the two regimes occurs when $\omega_D \tau / n \approx \pi$, i.e., $\tau' \approx n\pi$, leading to $F_n(\tau') \sim \mathcal{O}(1)$. This is indicated by the horizontal lines in Figs. 1(a) and 1(b), designating $\tau' = \tau'_{F=1}$, where $F_n(\tau') = 1$.

With these considerations in mind, appropriate scaling of OFDD sequences for a given experimental setting (i.e., an effective measurement of ω_D) can be accomplished experimentally using a feedback routine as follows: (1) Numerically calculate the OFDD set for n pulses in dimensionless units over a time domain $[0, 2\tau'_{F=1}]$. (2) Measure the coherence time τ_c, i.e., the time for the error to increase to $1/e$ of its asymptotic value, for the n-pulse sequence, e.g., using CPMG or UDD. (3) Associate the pulse sequence [obtained in (1)] at $\tau'_{F=1}$ with the measured τ_c as a first estimate of the scaling. (4) Find the sequence in the OFDD set that optimally suppresses errors for $\tau = \tau_c$ using a one-dimensional search algorithm and experimental feedback. Only a single sequence in the set should provide optimum error suppression when the τ_c is chosen as the sequence duration since the sequences are locally optimized. (5) Scale the duration of all sequences in the set using the result of the above optimization.

In the above prescription, a single-parameter feedback algorithm, implemented at only one choice of sequence duration, simultaneously determines the scaling of all sequences within an analytically derived OFDD set. This stands in contrast to the n-dimensional feedback optimization routine (for n pulses) used in our earlier work [12] as a means of finding optimized sequences, and which must be repeated for each choice of sequence duration.

The generality of the OFDD approach discussed so far applies strictly only to the instantaneous π-pulse limit. When the pulse durations are nonzero and comparable to the inverse cutoff frequency, the relative time scale of τ_π-to-$1/\omega_D$—possibly an experimental unknown—enters the problem. However, we find empirically that (up to $\omega_D \tau_\pi \approx 1$) the pulse sequences obtained by accounting for τ_π in minimizing $A_F(\tau')$ are nearly the same set of sequences as shown in Fig. 1, but contracted along the τ' axis as compared to the instantaneous pulse case. Hence the two scenarios differ primarily in the same scaling factor that the feedback is designed to determine, and the technique still works. After scaling, significant deviation between the instantaneous and finite-duration cases occurs only at short times, when the total free-precession time is comparable to $n\tau_\pi$, but there the error suppression is extremely strong for any dynamical decoupling approach.

We use $^9Be^+$ ions in a Penning trap as a model qubit system to demonstrate the proposed dynamical decoupling scheme. We present only a brief summary of our experimental system, as it has been described in detail elsewhere [12,13,16]. A few hundred to a few thousand ions are trapped and Doppler laser cooled to ~ 1 mK. The ~ 124 GHz (at 4.5 T), $2s^2S_{1/2}|m_I = 3/2, m_J = -1/2\rangle = |\downarrow\rangle \rightarrow |m_I = 3/2, m_J = +1/2\rangle = |\uparrow\rangle$ spin-flip transition of $^9Be^+$ serves as a qubit. Coherent rotations of the qubit are induced by a microwave field, producing a tunable Rabi flopping π-pulse duration, here 229 μs.

Each experiment begins by optically pumping all ions into the state ($|\uparrow\rangle$) which is bright to cooling light fluorescence. The qubits are then rotated to lie along the y axis by applying a $\pi/2$ pulse before initiating the decoupling sequence. The decoupling sequence ends with a $\pi/2$ pulse that in the absence of dephasing rotates the qubits to the dark state ($|\downarrow\rangle$). The accumulation of phase errors is manifested as nonzero fluorescence at the end of the experiment, due to a nonzero probability of qubit population in $|\uparrow\rangle$. The normalized fluorescence count rate measured after application of a decoupling sequence is a measure of this error and is given by $[1 - W(\tau)]/2$. We achieve a minimum combined operational and measurement fidelity of $\sim 99\%$ for sequences with $n \lesssim 10$. A desired noise environment is synthesized by frequency modulating the microwave drive as explained in [13].

Figure 3 compares the experimental performance of different decoupling sequences measured in (a) the ambient noise environment of our trap, which approximately scales as $\sim 1/\omega^4$ [12,13], (b) and (c) a synthesized Ohmic spectrum with a sharp cutoff around 500 Hz and 250 Hz, respectively. We use here the OFDD sequences shown in

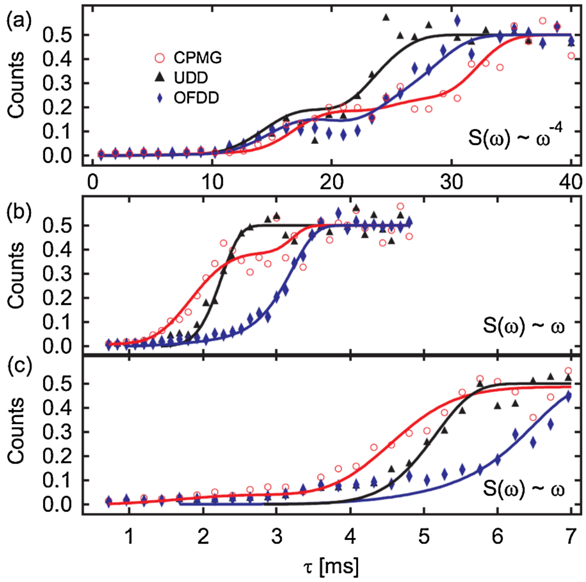

FIG. 3 (color online). Time evolution of the normalized fluorescence counts, equivalent to $[1 - W(\tau')]/2$, measured using $^9Be^+$ qubits in a Penning ion trap in (a) the ambient noise environment and a synthesized Ohmic noise environment with (b) a frequency cutoff near 500 Hz and (c) a frequency cutoff near 250 Hz. We used 6 π pulses in each sequence and open circles represent CPMG, triangles UDD, and diamonds OFDD. The data are well described by the fits (solid lines) which use the analytical expression for the coherence, the measured noise spectra in both environments, and the noise strength as a free parameter. We are at this time unsure of the cause of the minor discrepancy between the fits and the UDD and OFDD data in (c). This may be the consequence of external noise influences not accounted for in the synthesized spectrum.

Fig. 1(a), having subdivided the interval $0 < \tau' < 30$ into about 3000 intervals. After measuring a 6 π-pulse CPMG error curve we choose for each spectrum a fixed sequence duration $\tau \approx \tau_c$ ($\tau = 20$ ms, 2.8 ms and 5.5 ms, respectively) and perform a golden-section search with experimental feedback to determine which OFDD sequence of the set gives optimum error suppression for the selected τ. The feedback algorithm converges to the optimized sequence within ~10 iterations. (More specifically to a narrow band of sequences all of which give an error indistinguishable within the measurement noise. This band can in principle be made arbitrarily narrow with sufficient averaging during measurement.) This fixes the appropriate sequence associated with any other choice of τ. As anticipated from the simulations presented earlier, we obtain comparable results for the different decoupling techniques in the ambient noise environment with a soft high-frequency cutoff, Fig. 3(a). By contrast, in the Ohmic noise environment with a sharp cutoff around 500 Hz, Fig. 3(b), the OFDD sequence shows significant improvements over the other sequences even in the low-fidelity regime (decoherence >1%). To illustrate that the feedback algorithm finds the appropriate scaling for arbitrary cutoff we decrease the cutoff by a factor of 2 and repeat the experiment, Fig. 3(c). This increases the coherence time of the system and the benefit due to OFDD remains. Note that despite having finite-duration π-pulses $\omega_D \tau_\pi \approx 0.7$ the technique still works for reasons explained earlier.

In conclusion, we have presented a dynamical decoupling technique designed for optimized noise filtration by enforcing an analytical condition that does not rely on any detailed knowledge of the noise power spectrum. The technique significantly reduces the burden of performing measurement-feedback-based optimization of decoupling sequences [12], as it relies on only a single parameter search at one point of the error curve. Under appropriate conditions it improves error suppression by several orders of magnitude compared to those of standard sequences. Experimental measurements using a model quantum system and artificially engineered noise environments validate the predicted performance of these sequences.

We thank W. M. Itano, N. Shiga and A. P. VanDevender for contributions to hardware and software developments, and Y. Colombe and D. Hume for helpful comments on the manuscript. M. J. B. acknowledges support from IARPA and Georgia Tech., and H. U. acknowledges support from the CSIR. This Letter is a contribution of NIST, not subject to U.S. copyright.

[1] L. Viola and S. Lloyd, Phys. Rev. A **58**, 2733 (1998).
[2] D. Vitali and P. Tombesi, Phys. Rev. A **59**, 4178 (1999).
[3] G. S. Uhrig, Phys. Rev. Lett. **98**, 100504 (2007).
[4] L. Cywinski *et al.*, Phys. Rev. B **77**, 174509 (2008).
[5] G. S. Uhrig, New J. Phys. **10**, 083024 (2008).
[6] L. Viola, E. Knill, and S. Lloyd, Phys. Rev. Lett. **82**, 2417 (1999).
[7] G. Gordon, G. Kurizki, and D. A. Lidar, Phys. Rev. Lett. **101**, 010403 (2008).
[8] K. Khodjasteh and L. Viola, Phys. Rev. Lett. **102**, 080501 (2009).
[9] E. Hahn, Phys. Rev. **80**, 580 (1950).
[10] K. Khodjasteh and D. A. Lidar, Phys. Rev. Lett. **95**, 180501 (2005).
[11] L. M. K. Vandersypen and I. L. Chuang, Rev. Mod. Phys. **76**, 1037 (2005).
[12] M. J. Biercuk, H. Uys, A. P. VanDevender, N. Shiga, W. M. Itano, and J. J. Bollinger, Nature (London) **458**, 996 (2009).
[13] M. J. Biercuk, H. Uys, A. P. VanDevender, N. Shiga, W. M. Itano, and J. J. Bollinger, Phys. Rev. A **79**, 062324 (2009).
[14] M. J. Madsen *et al.*, Phys. Rev. Lett. **97**, 040505 (2006).
[15] D. Press *et al.*, Nature (London) **456**, 218 (2008).
[16] M. J. Jensen, T. Hasegawa, and J. J. Bollinger, Phys. Rev. A **70**, 033401 (2004).